ARTICLE

Effects of Surface Passivation on Twin-Free GaAs Nanosheets

Shermin Arab,[‡,⊥] Chun-Yung Chi,[‡,⊥] Teng Shi,[||] Yuda Wang,[||] Daniel P. Dapkus,[†,‡,§,⊥] Howard E. Jackson,[||] Leigh M. Smith,[||] and Stephen B. Cronin*[,†,‡,⊥]

[†]Department of Physics, [‡]Department of Electrical Engineering, [§]Department of Chemical Engineering and Materials Science, and [⊥]Center for Energy Nanoscience, University of Southern California, Los Angeles, California 90089, United States and [||]Department of Physics, University of Cincinnati, Cincinnati, Ohio 45221, United States

ABSTRACT Unlike nanowires, GaAs nanosheets exhibit no twin defects, stacking faults, or dislocations even when grown on lattice mismatched substrates. As such, they are excellent candidates for optoelectronic applications, including LEDs and solar cells. We report substantial enhancements in the photoluminescence efficiency and the lifetime of passivated GaAs nanosheets produced using the selected area growth (SAG) method with metal organic chemical vapor deposition (MOCVD). Measurements are performed on individual GaAs nanosheets with and without an AlGaAs passivation layer. Both steady-state photoluminescence and time-resolved photoluminescence spectroscopy are performed to study the optoelectronic performance of these nanostructures. Our results show that AlGaAs passivation of GaAs nanosheets leads to a 30- to 40-fold enhancement in the photoluminescence intensity. The photoluminescence lifetime increases from less than 30 to 300 ps with passivation, indicating an order of magnitude improvement in the minority carrier lifetime. We attribute these enhancements to the reduction of nonradiative recombination due to the compensation of surface states after passivation. The surface recombination velocity decreases from an initial value of 2.5×10^5 to 2.7×10^4 cm/s with passivation.

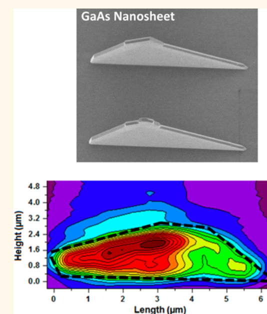

KEYWORDS: MOCVD · GaAs · nanosheet · photoluminescence · lifetime · AlGaAs

GaAs is an excellent candidate material for high efficiency solar cells,[1,2] nanolasers[3,4] and LED applications.[5] GaAs nanostructures (*e.g.*, nanowires and nanosheets) with high surface-to-volume ratios, however, suffer from high surface state densities and high surface recombination velocities, which typically limit their optoelectronic device performance.[6] Passivation of GaAs nanostructures has been widely studied in the literature, including cladding of GaAs nanostructures with wide gap materials (*e.g.*, AlGaAs, GaP and GaAsP).[3,5,7−9] A number of chemical routes to passivation of GaAs surfaces have been studied, including sulfur solution passivation,[10,11] thiol passivation,[12] and ionic liquid passivation.[13] Recently, selective area growth (SAG) of GaAs nanosheets has been demonstrated using a slit instead of a hole geometry in the SiN growth masking layer.[14] GaAs nanosheets have the distinct advantage over GaAs nanowires in that they grow easily without the formation of twin defects and stacking faults, thus improving the overall sample quality and optoelectronic properties in comparison to GaAs nanowires.[15] Longer minority carrier diffusion lengths make GaAs nanosheets particularly well-suited for solar cell and nanolaser applications. Previous literature provides extensive studies on AlGaAs passivation of GaAs nanowires.[16,17] However, no such studies have been reported for GaAs nanosheets.

In the work presented here, the effects of passivation of GaAs nanosheet structures are explored using heteroepitaxial growth of an AlGaAs passivation layer on the GaAs nanosheet. The effects of passivation on the photoluminescence efficiency and minority carrier lifetimes are studied systematically using the techniques of room temperature and low temperature photoluminescence (PL) spectroscopy and time-resolved photoluminescence (TRPL) spectroscopy. All measurements are performed on individual GaAs nanosheets that have been removed from the growth substrate and transferred to Si/SiO_2 substrates in order to eliminate any contribution to the PL from the underlying substrate.

RESULTS AND DISCUSSION

Figure 1a shows an SEM image of the as-grown nanosheets on the underlying GaAs/SiN growth substrate. The nanosheets are then removed by sonication in IPA and deposited on a Si/SiO_2 substrate, as shown

* Address correspondence to scronin@usc.edu.

Received for review September 15, 2014 and accepted January 7, 2015.

Published online January 07, 2015
10.1021/nn505227q

© 2015 American Chemical Society

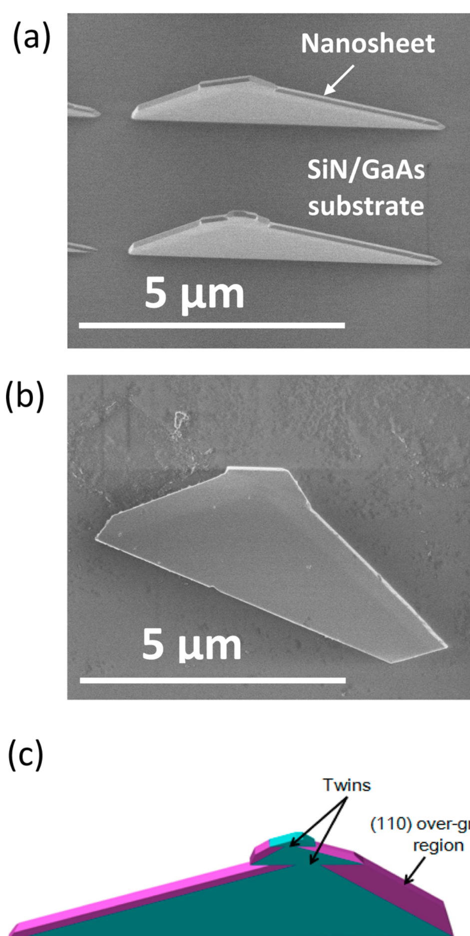

Figure 1. SEM images of nonpassivated GaAs nanosheet: (a) array of as-grown nanosheets, (b) individual nanosheet deposited on Si/SiO_2 substrate, and (c) schematic diagram of the GaAs nanosheet structure.

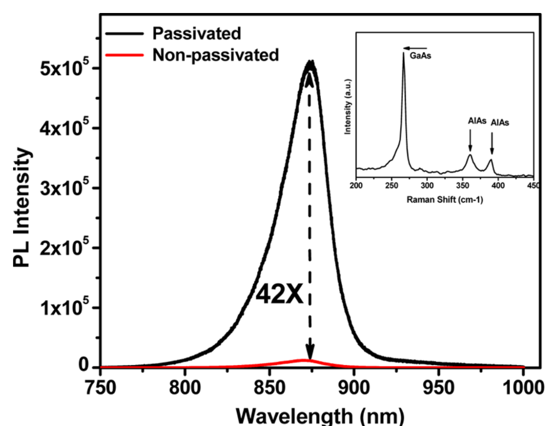

Figure 2. Photoluminescence spectra of an individual GaAs nanosheet with and without AlGaAs passivation. Inset graph: Raman spectra of passivated GaAs nanosheet.

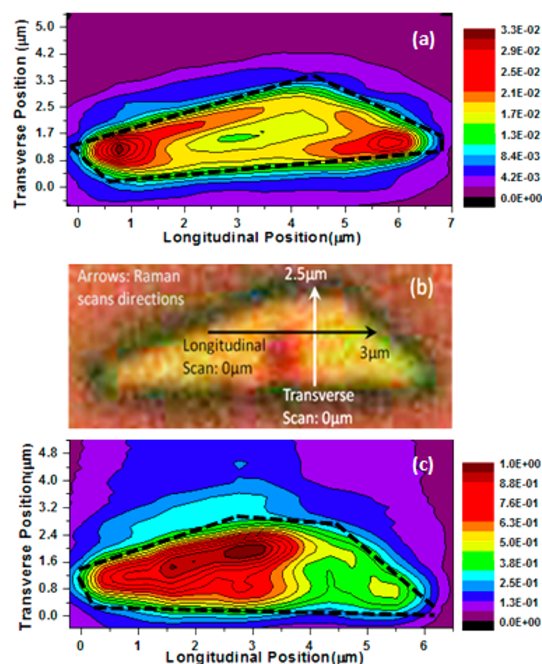

Figure 3. Spatial maps of the PL intensity: (a) PL spatial map for an as-grown and thus unpassivated GaAs nanosheet (maximum PL intensities for white area to minimum PL intensity at dark purple area). (b) Optical image of the nanosheet passivated with a 20 nm AlGaAs layer, where the arrows show the direction of the line scans used for spatially resolved micro-Raman measurements shown later. (c) PL spatial map for the passivated GaAs/AlGaAs nanosheet.

in Figure 1b. A schematic diagram of the nanosheet structure is shown in Figure 1c. Nanosheets are grown along the (111) direction through a self-terminating process. The base triangle is referred to as the initial growth region of the nanosheet. Once the initial triangle self-terminates, additional triangles may grow from the apex of the initial triangle, which is referred to as the overgrown region.[14,15] In these nanosheet structures, the exposed surface of the nanosheet is the (011) plane. In the subsequent passivation growth step, AlGaAs is grown on this surface, which is not the usual surface for epitaxial growth. It is, therefore, not known *a priori* how epitaxial the GaAs/AlGaAs interface will be in these novel nanostructures, thus providing additional motivation for this study.

Figure 2 shows a comparison of the PL spectra taken at a single point from an individual nanosheet with and without AlGaAs passivation. Nanosheets are excited with 532 nm wavelength (continuous wave) laser light at room temperature with a 100× objective lens. Here, the PL intensity is enhanced by a factor of 42× after AlGaAs passivation. We have measured over 30 samples of passivated and nonpassivated GaAs nanosheets, from separate runs. Our results indicate an average of 30- to 40-fold enhancement in PL intensity after AlGaAs passivation. To assess how the passivation of the nanosheet might affect the spatial distribution of PL, spatial maps of the PL intensity were obtained using slit-confocal microscopy. Figure 3a shows such a spatial map where the integrated intensity of the band-edge emission is displayed as a function of position for an as-grown and, thus, unpassivated GaAs nanosheet. One can see points of relatively bright emission at the two ends of the nanosheet, while the interior of the

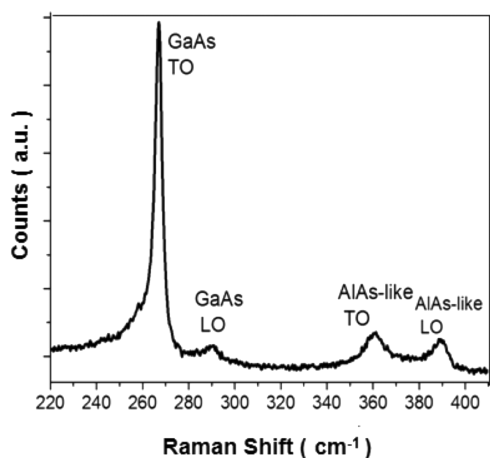

Figure 4. Selected Raman spectrum near the center of the GaAs/AlGaAs sample. GaAs TO (267 cm^{-1}) and AlAs-like TO (360 cm^{-1}) and LO (388 cm^{-1}) phonon structures are clearly identified, along with a weak GaAs LO response (~290 cm^{-1}). The weak structure at the lower energy side of the GaAs TO is presumably GaAs-like TO response from AlGaAs.

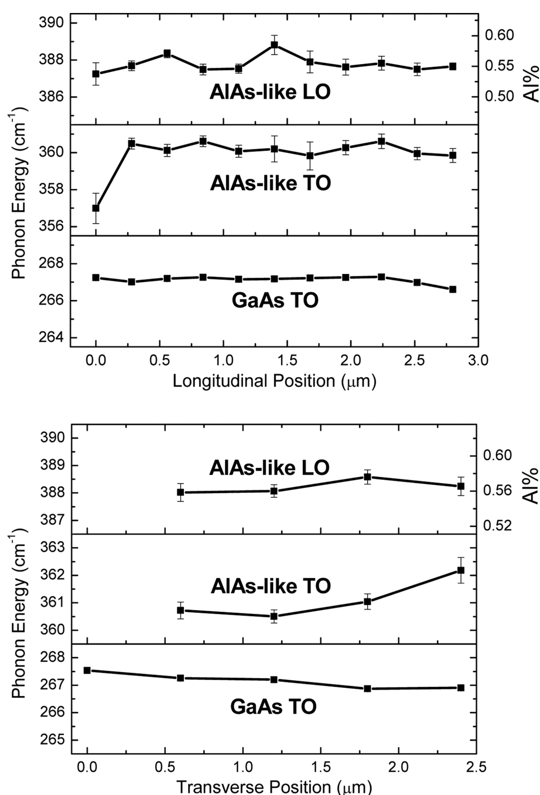

Figure 5. Longitudinal and transverse Raman scattering scan analysis. The Al-concentration is calculated based on AlAs-like LO phonon energy due to its strong Al-concentration dependent nature.[22] From both of the scans, we observe a consistent Al-concentration 50% across the sample with a deviation of ~2%.

nanosheet emits at approximately 30−50% the maximum intensity. Figure 3b shows an optical image of the nanosheet passivated with a 20 nm AlGaAs layer, where the arrows show the direction of the line scans used for spatially resolved micro-Raman measurements shown later. Figure 3c shows a PL image of the passivated GaAs/AlGaAs nanosheet. By comparing the two PL images in Figure 3a and 3c, we find that the maximum intensity integrated over the whole area of the passivated GaAs nanosheet is nearly 30 times that of the unpassivated nanosheet. The fact that the PL intensity maximum occurs along the intermediate edge may indicate that the AlGaAs-on-GaAs growth is higher quality at this edge. One should also consider the fact that near the edge the emission can couple out of the nanosheet more effectively. This is not surprising considering that this is the last surface deposited during the initial nanosheet growth. The weak PL intensity along the long edge indicates that the long edge is not passivated since it is cleaved from the growth substrate.

To assess whether the reduced intensity at a position in the passivated nanosheet is due to an imperfection or inhomogeneity in the AlGaAs layer, we perform spatially resolved micro-Raman spectroscopy on the same nanosheet. The 514.5 nm line from an argon-ion laser is used for excitation with 0.5 mW power and the scattered light is collected by a 100× 0.7NA objective lens. The scattered light is dispersed by an *xy*-Dilor spectrometer and detected by a liquid-nitrogen cooled Si-CCD. The sample is mounted on a piezoelectric translation stage so that the nanosheet can be sampled along two orthogonal lines, longitudinal and transverse, as shown in the optical image of the nanosheet (Figure 3a). The Raman spectra (see Figure 4) reveal GaAs-like TO, AlAs-like TO and LO features, along with a weak GaAs-like LO response. These phonon energies are obtained by fitting the Raman spectra to Lorentzian lineshapes for both scans, as displayed in Figure 5a,b for the longitudinal and transverse line scans, respectively. Since the position of the AlAs-like LO phonon is a sensitive measure of Al concentration,[19] we obtained the Al% based on the observed phonon energies using the equation:

$$\omega_{LO} = 361.643 + 62.888x - 27.91x^2$$

Here, x is the percentage of Al concentration and ω_{LO} is the AlAs-like LO phonon. We find the Al% is consistently 55% across the entire area of the nanosheet, with only a small deviation of 1%, indicating good growth quality and control across the sample. As such, there is no obvious correlation of the reduced region of PL intensity with the concentration of the AlGaAs layer. In our previous work on AlGaAs passivated GaAs nanowires, we found that PL intensity was strongly correlated with the thickness of AlGaAs layer.[7] For AlGaAs passivated GaAs nanosheet, atomic force microscopy (AFM) does not show obvious variation of thickness. Hence, we believe that the variation in PL intensity is largely due to poor epitaxial growth at the interface of GaAs/AlGaAs or possible surface defects.

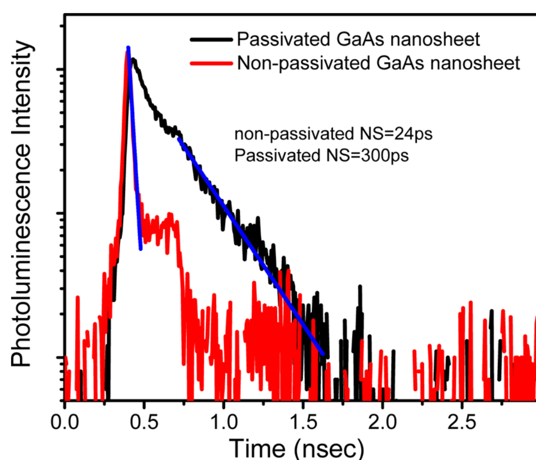

Figure 6. Time resolved PL data from passivated and unpassivated GaAs nanosheets at 300 K. The nonpassivated GaAs nanosheet PL lifetime is less than the system response (30 ps). The passivated nanosheet PL exhibits a lifetime of 300 ps.

Time-resolved PL spectroscopy was also performed on these nanosheets in order to determine the carrier lifetimes before and after passivation, as shown in Figure 6. We find that passivation of n-type GaAs nanosheets with an AlGaAs layer yields carrier lifetimes of up to 300 ps, which is an order of magnitude longer than the nonpassivated nanosheets with a lifetime of less than 30 ps, which is our system response. The increase in carrier lifetime is due to passivation of the surface states, which greatly reduces the nonradiative recombination of photoexcited carriers. Given the 30-fold increase in PL intensity seen in the PL maps of Figure 3, we infer that the unresolved recombination lifetime in the unpassivated nanosheet may be only ∼10 ps and is limited by the nonradiative recombination at the surfaces. This result is consistent with previous reports of GaAs nanowires passivated with AlGaAs,[7] which showed a lifetime of 1.3 ns for AlGaAs-passivated nanowires. A direct comparison is not possible, however, since the doping levels of both structures are unknown. The surface recombination velocity (SRV) can be approximated using the following formula:[6,20]

$$\frac{1}{\tau} = \frac{1}{\tau_b} + \frac{4S}{d}$$

Here, τ is the minority carrier lifetime, τ_b is the bulk GaAs lifetime (1.3 μs), d is the thickness of the nanosheets, and S is the surface recombination velocity. Considering a GaAs nanosheet with an average thickness of 300 nm, the surface recombination velocity measured for an AlGaAs-passivated sample is 2.7×10^4 cm/s, which is about an order of magnitude smaller than the value measured for the nonpassivated case of greater than 2.5×10^5 cm/s). Lower SRV values of 500 cm/s have been reported for passivated bulk GaAs in the literature.[21] The fact that our result is 4 times higher than the minimum value reported may be attributed to the fact that the passivation growth is not optimized.

CONCLUSION

In conclusion, our steady-state and time-resolved photoluminescence measurements of individual GaAs nanosheets indicate that AlGaAs passivation improves the photoluminescence efficiency by 30–40 times and increases the minority carrier lifetime by more than an order of magnitude. We attribute these enhancements to the reduction of nonradiative recombination due to the compensation of surface states after passivation. The surface recombination velocity shows a drastic decrease from 2.5×10^5 to 2.7×10^4 cm/s. These results indicate that passivated GaAs nanosheets have superior optoelectronic properties with longer-lived carriers than nonpasivated GaAs nanosheets.

METHODS

GaAs nanosheets are synthesized in a vertical showerhead, low-pressure metal organic chemical vapor deposition (MOCVD) reactor with selective area growth (SAG).[14,15] Trimethylgallium (TMGa), trimethylaluminum (TMAl), and arsine are used as precursors for Ga, Al, and As deposition. Nanosheets are doped n-type using disilane (Si_2H_6). High density arrays of GaAs nanosheets are grown on (111)B GaAs substrates. The substrate preparation for nanosheet growth is the same as that previously reported.[14] First, a thin layer of SiN_x (approximately 28 nm thick) is deposited onto the (111)B GaAs substrate by plasma enhanced chemical vapor deposition (PECVD). Ten μm long, 100 nm wide openings are patterned in the SiN_x layer by electron-beam lithography and reactive ion etching. These nanoscale stripes are patterned along the $\langle 11\bar{2} \rangle$ direction of the GaAs growth substrate. The nanosheets are grown in a hydrogen environment at 0.1 atm using a V/III ratio of 1.5 and a Ga/Si ratio of 16 000 for 75 min at 790 °C. The partial pressures of TMGa, AsH_3, and Si_2H_6 were 1.12×10^{-6}, 1.63×10^{-6}, and 7.14×10^{-11} atm, respectively. The AlGaAs passivation layer is grown at the same temperature for 150 s with TMGa, AsH_3, and TMAl at partial pressures of 3.74×10^{-7}, 1.85×10^{-4}, and 3.82×10^{-7} atm. The approximate thickness of the AlGaAs passivation layer is 20 nm, while that of the nanosheets is 300 nm, as measured by scanning electron microscopy (SEM) and atomic force microscopy (AFM). The GaAs nanosheets in this study do not have a GaAs capping layer. Nevertheless, the optical behavior of these nanosheets is found to be sable over a 3-month period.

Micro-Raman spectroscopy of the nanosheets was performed using a 100× objective lens with a numerical aperture of 0.85 and a 40× objective lens with a numerical aperture of 0.6. A Si CCD camera was used to collect PL spectra in the 750–1000 nm wavelength range. A continuous wave, 514 or 532 nm laser was used for excitation. For the time-resolved PL measurements, a 76 MHz pulsed Ti-Sapphire laser (Mira 900) was used to pump a supercontinuum fiber and provide optical excitation at 590 nm. The 590 nm excitation light was focused onto the nanosheet using a 50×/0.5NA objective lens, and the emitted PL was dispersed by a MS260i (Newport) imaging spectrograph and detected by a MCP-PMT (Hamamatsu) photo-tube. Time-correlated single photon counting was used to obtain time-resolved PL data. Spatial imaging of single nanosheets was

obtained using slit-confocal microscopy.[18] The 514 nm laser was defocused to a ~30 μm spot (encompassing the full nanosheet), while the nanosheet was imaged with the short axis of the nanosheet oriented parallel to the entrance slit of the spectrometer. As the nanosheet was scanned across the entrance slit along the long axis, full CCD images of the PL were obtained,

Conflict of Interest: The authors declare no competing financial interest.

Acknowledgment. This material is based upon work supported as part of the Center for Energy Nanoscience (CEN), an Energy Frontier Research Center (EFRC) funded by the U.S. Department of Energy, Office of Science and Office of Basic Energy Sciences, under Award DE-SC0001013. We also acknowledge the National Science Foundation through DMR-1105362, 1105121 and ECCS-1100489.

REFERENCES AND NOTES

1. Geisz, J.; Kurtz, S.; Wanlass, M.; Ward, J.; Duda, A.; Friedman, D.; Olson, J.; McMahon, W.; Moriarty, T.; Kiehl, J. High-Efficiency GaInP/GaAs/InGaAs Triple-junction Solar Cells Grown Inverted with a Metamorphic Bottom Junction. *Appl. Phys. Lett.* **2007**, *91*, No. 023502.
2. Woodall, J.; Hovel, H. High-Efficiency Ga1− xAlxAs−GaAs Solar Cells. *Appl. Phys. Lett.* **1972**, *21*, 379–381.
3. Hua, B.; Motohisa, J.; Kobayashi, Y.; Hara, S.; Fukui, T. Single GaAs/GaAsP Coaxial Core−Shell Nanowire Lasers. *Nano Lett.* **2008**, *9*, 112–116.
4. Saxena, D.; Mokkapati, S.; Parkinson, P.; Jiang, N.; Gao, Q.; Tan, H. H.; Jagadish, C. Optically Pumped Room-temperature GaAs Nanowire Lasers. *Nat. Photonics* **2013**, *7*, 963–968.
5. Tomioka, K.; Motohisa, J.; Hara, S.; Hiruma, K.; Fukui, T. GaAs/AlGaAs Core Multishell Nanowire-Based Light-emitting Diodes on Si. *Nano Lett.* **2010**, *10*, 1639–1644.
6. Nelson, R.; Sobers, R. Interfacial Recombination Velocity in GaAlAs/GaAs Heterostructures. *Appl. Phys. Lett.* **2008**, *32*, 761–763.
7. Chang, C.-C.; Chi, C.-Y.; Yao, M.; Huang, N.; Chen, C.-C.; Theiss, J.; Bushmaker, A. W.; LaLumondiere, S.; Yeh, T.-W.; Povinelli, M. L. Electrical and Optical Characterization of Surface Passivation in GaAs Nanowires. *Nano Lett.* **2012**, *12*, 4484–4489.
8. Noborisaka, J.; Motohisa, J.; Hara, S.; Fukui, T. Fabrication and Characterization of Freestanding GaAs/AlGaAs Core-Shell Nanowires and AlGaAs Nanotubes by Using Selective-Area Metalorganic Vapor Phase Epitaxy. *Appl. Phys. Lett.* **2005**, *87*, No. 093109.
9. Titova, L.; Hoang, T. B.; Jackson, H.; Smith, L.; Yarrison-Rice, J.; Kim, Y.; Joyce, H.; Tan, H.; Jagadish, C. Temperature Dependence of Photoluminescence from Single Core-Shell GaAs−AlGaAs Nanowires. *Appl. Phys. Lett.* **2006**, *89*, 173123–173126.
10. Sandroff, C.; Hegde, M.; Farrow, L.; Chang, C.; Harbison, J. Electronic Passivation of GaAs Surfaces through the Formation of Arsenic-sulfur Bonds. *Appl. Phys. Lett.* **1989**, *54*, 362–364.
11. Liu, D.; Zhang, T.; LaRue, R.; Harris, J., Jr; Sigmon, T. Deep Level Transient Spectroscopy Study of GaAs Surface States Treated with Inorganic Sulfides. *Appl. Phys. Lett.* **1988**, *53*, 1059–1061.
12. Lunt, S. R.; Ryba, G. N.; Santangelo, P. G.; Lewis, N. S. Chemical Studies of the Passivation of GaAs Surface Recombination Using Sulfides and Thiols. *J. Appl. Phys.* **1991**, *70*, 7449–7467.
13. Arab, S.; Anderson, P. D.; Yao, M.; Zhou, C.; Dapkus, P. D.; Povinelli, M. L.; Cronin, S. B. Enhanced Fabry-Perot Resonance in GaAs Nanowires through Local Field Enhancement and Surface Passivation. *Nano Res.* **2014**, *7*, 1146–1153.
14. Chi, C.-Y.; Chang, C.-C.; Hu, S.; Yeh, T.-W.; Cronin, S. B.; Dapkus, P. D. Twin-Free GaAs Nanosheets by Selective Area Growth: Implications for Defect-Free Nanostructures. *Nano Lett.* **2013**, *13*, 2506–2515.
15. Chang, C.-C.; Chi, C.-Y.; Chen, C.-C.; Huang, N.; Arab, S.; Qiu, J.; Povinelli, M. L.; Dapkus, P. D.; Cronin, S. B. Carrier Dynamics and Doping Profiles in GaAs Nanosheets. *Nano Res.* **2014**, *7*, 163–170.
16. Perera, S.; Fickenscher, M.; Jackson, H.; Smith, L.; Yarrison-Rice, J.; Joyce, H.; Gao, Q.; Tan, H.; Jagadish, C.; Zhang, X. Nearly Intrinsic Exciton Lifetimes in Single Twin-Free GaAs/AlGaAs Core-Shell Nanowire Heterostructures. *Appl. Phys. Lett.* **2008**, *93*, No. 053110.
17. Jiang, N.; Gao, Q.; Parkinson, P.; Wong-Leung, J.; Mokkapati, S.; Breuer, S.; Tan, H. H.; Zheng, C.; Etheridge, J.; Jagadish, C. Enhanced Minority Carrier Lifetimes in GaAs/AlGaAs Core−Shell Nanowires through Shell Growth Optimization. *Nano Lett.* **2013**, *13*, 5135–5140.
18. Hewaparakrama, K.; Wilson, A.; Mackowski, S.; Jackson, H.; Smith, L.; Karczewski, G.; Kossut, J. Subwavelength Multichannel Imaging Using a Solid Immersion Lens: Spectroscopy of Excitons in Single Quantum Dots. *Appl. Phys. Lett.* **2004**, *85*, 5463–5465.
19. Wasilewski, Z.; Dion, M.; Lockwood, D.; Poole, P.; Streater, R.; SpringThorpe, A. Composition of AlGaAs. *J. Appl. Phys.* **1997**, *81*, 1683–1694.
20. Demichel, O.; Calvo, V.; Besson, A.; Noé, P.; Salem, B.; Pauc, N.; Oehler, F.; Gentile, P.; Magnea, N. Surface Recombination Velocity Measurements of Efficiently Passivated Gold-catalyzed Silicon Nanowires by a New Optical Method. *Nano Lett.* **2010**, *10*, 2323–2329.
21. Nelson, R. Interfacial Recombination in GaAlAs−GaAs Heterostructures. *J. Vac. Sci. Technol.* **1978**, *15*, 1475–1477.
22. Dobal, P.; Bist, H.; Mehta, S.; Jain, R. Laser Heating and Photoluminescence in GaAs and AlxGa1− xAs. *Appl. Phys. Lett.* **1994**, *65*, 2469–2471.